Construction of one-dimensional ZnCdS(EDA)/Ni@NiO for photocatalytic hydrogen evolution

Changyan Guo[a,#,*], Yangyang Zou[a,b,#], Yanqiu Ma[a], Naeem Akram[c], Ali Ahmad[c], and Jide Wang[a,*]

[a] Key Laboratory of Oil and Gas Fine Chemicals, Ministry of Education & Xinjiang Uygur Autonomous Region, School of Chemical Engineering and Technology, Xinjiang University, Urumqi, 830046, China.

[b] Coal Chemical Industry Technology Research Institute, China Energy Group Ningxia Industry Coal Co. Ltd., Yinchuan 750411, Ningxia, China.

[c] School of Chemical Engineering, Minhaj University Lahore, Lahore (54000) Pakistan.

[#] These authors contributed equally to this work.

* Corresponding author:

E-mail: gcyslw@xju.edu.cn (Changyan Guo); awangjd@sina.cn (Jide Wang).

1 Experimental sections

1.1 Materials and reagents

Cadmium nitrate tetrahydrate ($Cd(NO)_3 \cdot 4H_2O$), Zinc nitrate hexahydrate ($Zn(NO)_3 \cdot 6H_2O$), Thiourea (CH_4N_2S), Ethylenediamine($C_2H_8N_2$), Cobalt chloride ($NiCl_2 \cdot 6H_2O$), Sodium borohydride ($NaBH_4$), ethylene glycol $(CH_2OH)_2$. All reagents used were of analytical grade and used without further purification. Deionized water was used in all experiments.

1.2 Characterization and Instrumentation

The crystal structure of the samples was analyzed by Brook D8 X-ray diffractometer (XRD) at A scanning rate of 10°·min-1, 2θ range of 10°~ 80°, and Cu Kα radiation (=1.54178 Å). X-ray photoelectron spectroscopy (XPS) measurements were performed in a Thermo Fisher Scientific XPS ESCALAB 250 Xi instrument with an Al Kα (1486.8 eV) X-ray source to determine the valence states of all elements. The morphology of the sample was observed by field emission scanning electron microscope (FESEM) using Zeise Sigma 500 at 10 kV acceleration voltage. FEI Talos f200s transmission electron microscopy (HRTEM) was used to analyze the samples with high resolution under 200 kV acceleration voltage. Uv-vis measurements were performed on SHIMADZU UV-2600I using barium sulfate as a reference. The instrument used for ESR testing is the Bruker A300. BET performed nitrogen isothermal adsorption/desorption measurements on Micromeritics 3Flex. The samples were photoluminescence tested with Japanese HORIBA FluorOMax-4 at the same excitation wavelength. 1~2mg powder sample was taken and tested in an

infrared spectrometer (Nicolet is 5 FT-IR), with a wave number range of 4000~400cm^{-1}, scanning number of 32, and resolution of 4cm^{-1}.

1.3 Photocatalytic hydrogen production performance test

The 5 mg sample was dispersed in 10 mL of ultrapure water and subsequently transferred to a 20 mL photoreactor equipped with circulating water. The photoreactor was hermetically sealed and purged with argon for 10 minutes to eliminate any interference from air. To simulate the visible light source, a xenon lamp with a cut-off filter at 420 nm and power output of 300 W was employed. Gas chromatography (Japan Shimadzu Corporation GC-14B) equipped with a thermal conductivity detector (TCD) and a column packed with 5 Å sieves (4 mm × 2 m) was used for hourly analysis of the gas mixture, where only 100 μL were injected per hour. Argon served as the carrier gas.

1.4 Electrochemical test

All the electrochemical measurements were performed on a CHI660D electrochemical workstation (Shanghai Chenhua Instrument, Ltd. Shanghai, China) with a standard three-electrode system. The following methods were used to prepare working electrodes: 2 mg sample was put into a sample tube, and 480 μL of absolute ethanol and 20 μL of Nafion solution were added. The samples were dispersed by ultrasonic for 30min and then dropped on the prepared 1×1 cm^2 FTO (fluorine-doped tin-oxide) glass. The test frequency of electrochemical impedance spectroscopy (EIS) was 10^{-2} Hz to 10^4 Hz. All tests were performed at room temperature with 0.5 mol·L^{-1} Na_2SO_4 as electrolytes

Fig. S1. TEM Mapping of ZnCdS(EDA)

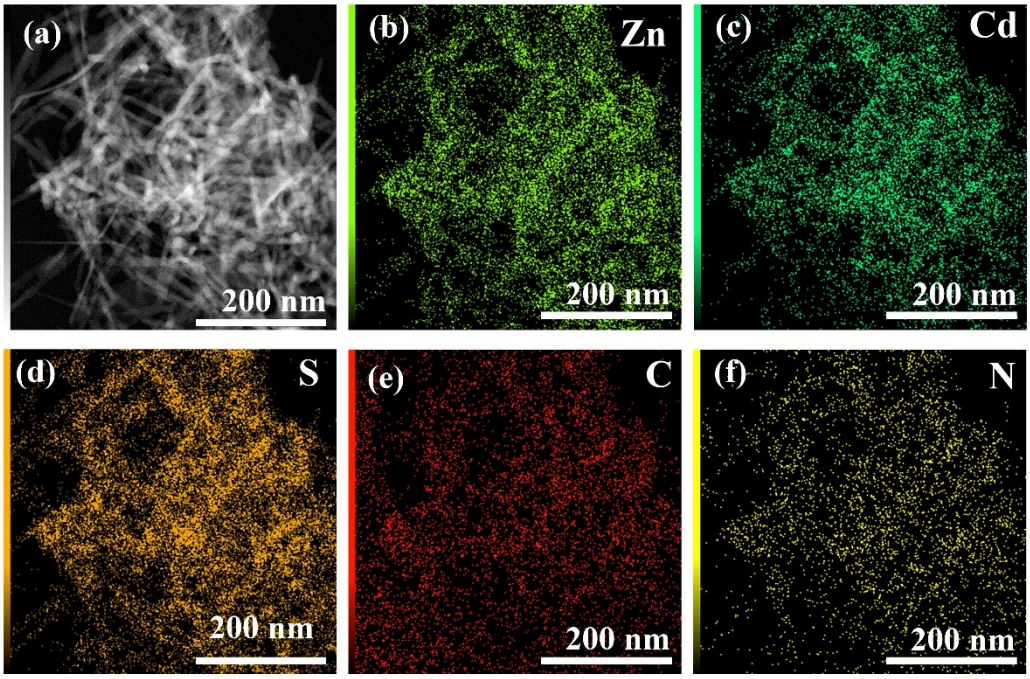

Fig. S1. TEM Mapping of ZnCdS(EDA)

Fig. S2. TEM Mapping of ZnCdS(WAT)

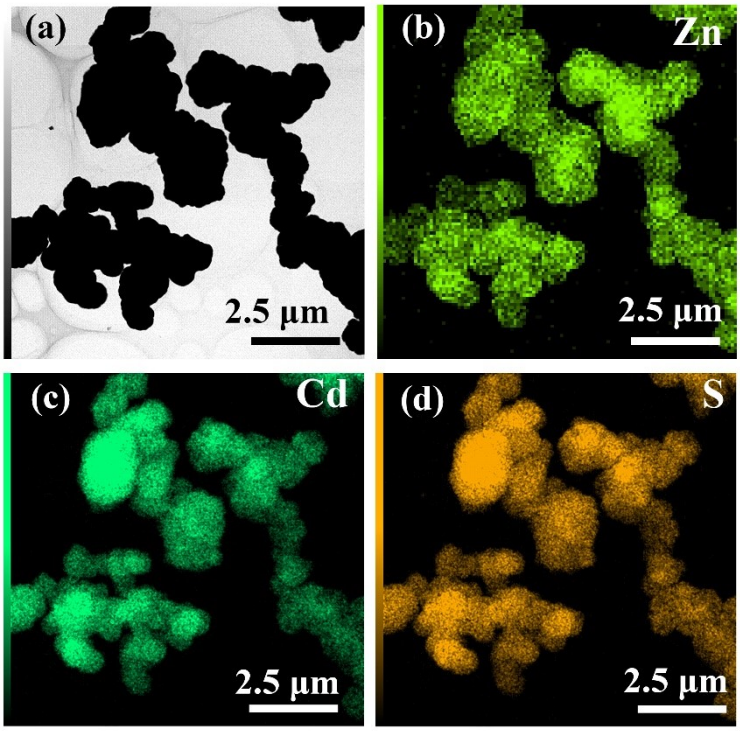

Fig. S2. TEM Mapping of ZnCdS(WAT).

Fig. S3. EDX of ZnCdS(EDA)/Ni@NiO

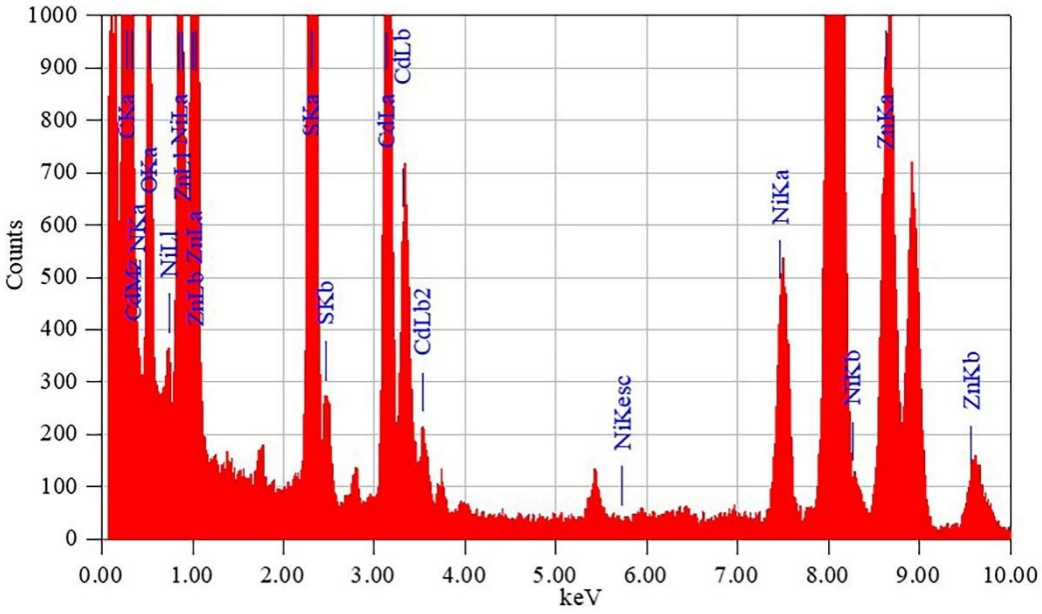

Fig. S3. EDX of ZnCdS(EDA)/Ni@NiO.

Fig. S4. Pore size distribution curves of several sampled

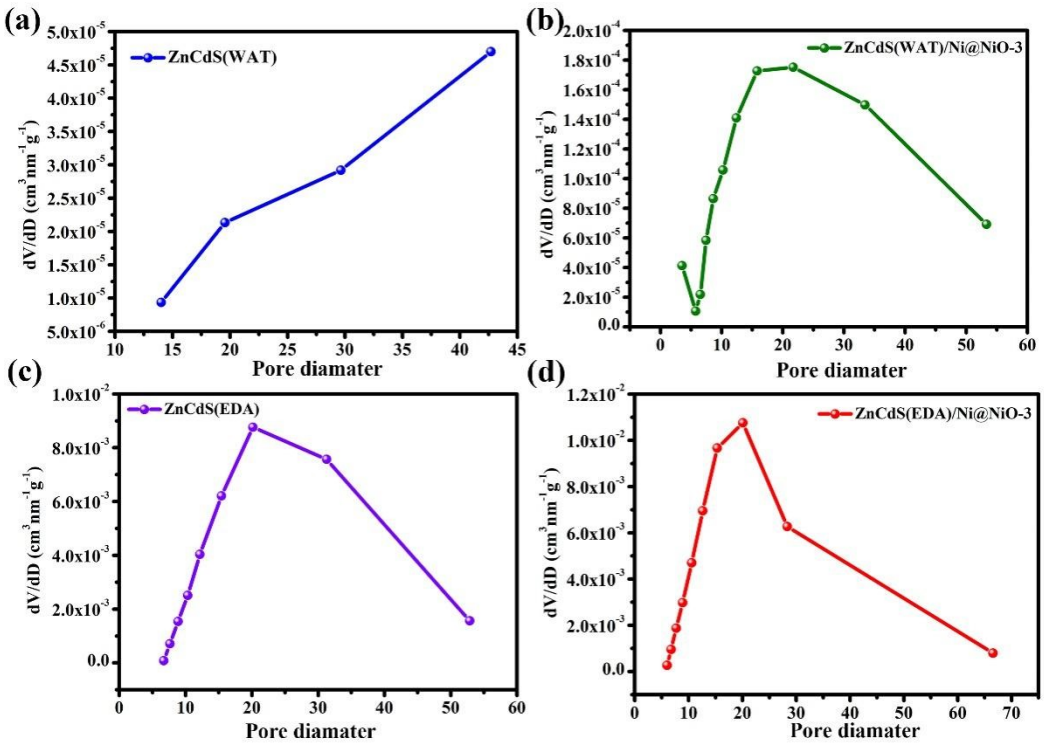

Fig. S4. Pore size distribution curves of several samples.

Fig. S5. Recycling in photocatalytic pure water splitting

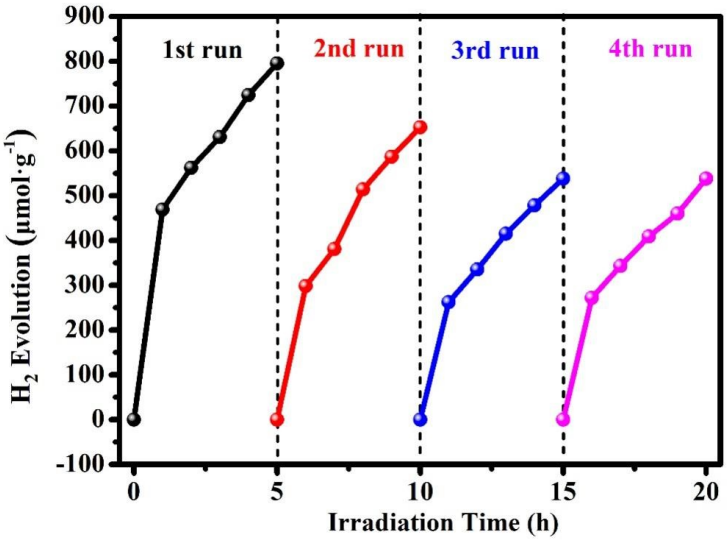

Fig. S5. Recycling performance of ZnCdS(EDA)/Ni@NiO-3 compounds in the sacrificial agent-free system.

Fig. S6. Recycling results in a mixed aqueous solution consisting of 9.5 mL water and 0.5 mL EDA system.

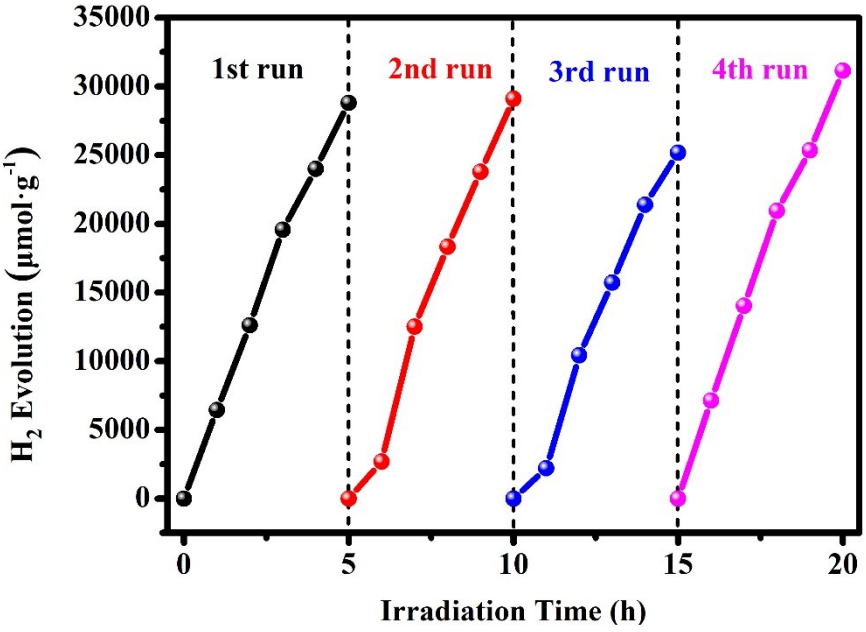

Fig. S6. Recycling results in a mixed aqueous solution consisting of 9.5 mL water and 0.5 mL EDA system.

Table S1. Hydrogen evolution performance of different catalysts under different conditions

Catalyst	Incident light	Catalytic system	H_2 evolution
ZnCdS(WAT)	Yes	9.5 mL water+0.5 mL EDA	Trace
ZnCdS(WAT)	Yes	10 mL water	Trace
ZnCdS(EDA)	Yes	9.5 mL water+0.5 mL EDA	70.45 $\mu mol \cdot g^{-1} \cdot h^{-1}$
ZnCdS(EDA)	Yes	10 mL water	Trace
ZnCdS(WAT)/Ni@NiO-3	Yes	9.5mL water+0.5 mL EDA	49.87 $\mu mol \cdot g^{-1} \cdot h^{-1}$
ZnCdS(WAT)/Ni@NiO-3	Yes	10 mL water	Trace
ZnCdS(EDA)/Ni@NiO-3	Yes	9.5 mLwater+0.5 mL EDA	5760.58 $\mu mol \cdot g^{-1} \cdot h^{-1}$
ZnCdS(EDA)/Ni@NiO-3	No	10 mL water	Trace
ZnCdS(EDA)/Ni@NiO-3	Yes	10 mL water	159.13 $\mu mol \cdot g^{-1} \cdot h^{-1}$

Table S2. Comparison of H_2 evolution performance over CdS-based photocatalysts

Photocatalyst	Incident light	H_2 evolution	Sacrificial agent	Ref.
$Zn_{0.5}Cd_{0.5}S$-P	≥420 nm	419.00 ($\mu mol \cdot h^{-1} \cdot g^{-1}$)	No	[1]
Pt-TiO_2/CdS	≥420 nm	3.07 ($\mu mol \cdot h^{-1} \cdot g^{-1}$)	No	[2]
CDs/CdS	≥420 nm	51.00 ($\mu mol \cdot h^{-1} \cdot g^{-1}$)	No	[3]
CdS/Ni_2P/g-C_3N_4	≥420 nm	15.56 ($\mu mol \cdot h^{-1} \cdot g^{-1}$)	No	[4]
Pt/CdS@Al_2O_3	≥420 nm	62.10 ($\mu mol \cdot h^{-1} \cdot g^{-1}$)	No	[5]
CoP/CdS/WS_2	≥420 nm	9.16 ($\mu mol \cdot h^{-1} \cdot g^{-1}$)	No	[6]
MoS_2/CdS	≥420 nm	145.00	No	[7]

		(μmol ·h^{-1} ·g^{-1})		
CdS-Pd (3.83‰)	≥420 nm	947.9 (μmol ·h^{-1} ·g^{-1})	No	[8]
ZnCdS(EDA)/Ni@ NiO	≥420 nm	159.13 (μmol ·h^{-1} ·g^{-1})	No	This work
Cd-NiS	≥420 nm	1.13 (mmol ·h^{-1} ·g^{-1})	0.35 M Na_2SO_3/ 0.25 M Na_2S	[9]
CdS-MoS_2-CoO_x	/	7.4 (mmol ·h^{-1} ·g^{-1})	TEOA	[10]
ZnO/CdS/ MoS_2	≥420 nm	10.25 (mmol ·h^{-1} ·g^{-1})	0.35 M Na_2SO_3/ 0.25 M Na_2S	[11]
AgBr/CdS	≥420 nm	5406 (μmol·g^{-1}·h^{-1})	TEOA	[12]
One-dimensional NiS/CdS	/	1.512 (mmol ·h^{-1} ·g^{-1})	Lignin/ Lactic acid	[13]
CdS/MoS_2	≥420 nm	1.36 (mmol ·h^{-1} ·g^{-1})	lactic acid	[14]
ZnO/CdS	/	4134 (μmol·g^{-1}·h^{-1})	0.35 M Na_2SO_3/ 0.25 M Na_2S	[15]
ZnCdS(EDA)/Ni@ NiO	≥420 nm	5760.58 (μmol·g^{-1}·h^{-1})	0.1 M Na_2SO_3/ 0.1 M Na_2S	This work

Fig. S7. XRD patterns of ZnCdS(EDA)/Ni@NiO-3

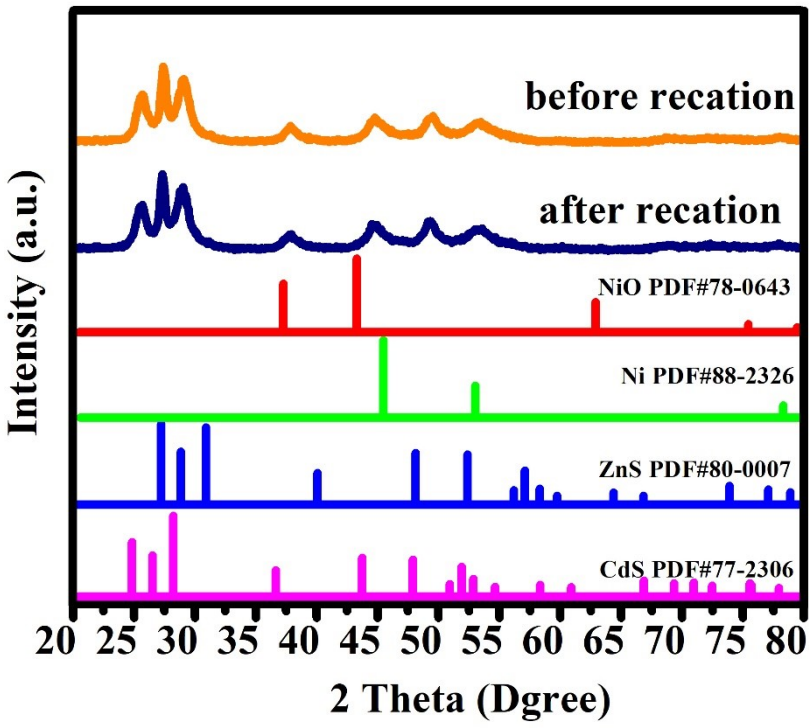

Fig. S7. XRD patterns of ZnCdS(EDA)/Ni@NiO-3.

Fig. S8. FTIR spectra of ZnCdS(EDA)/Ni@NiO-3

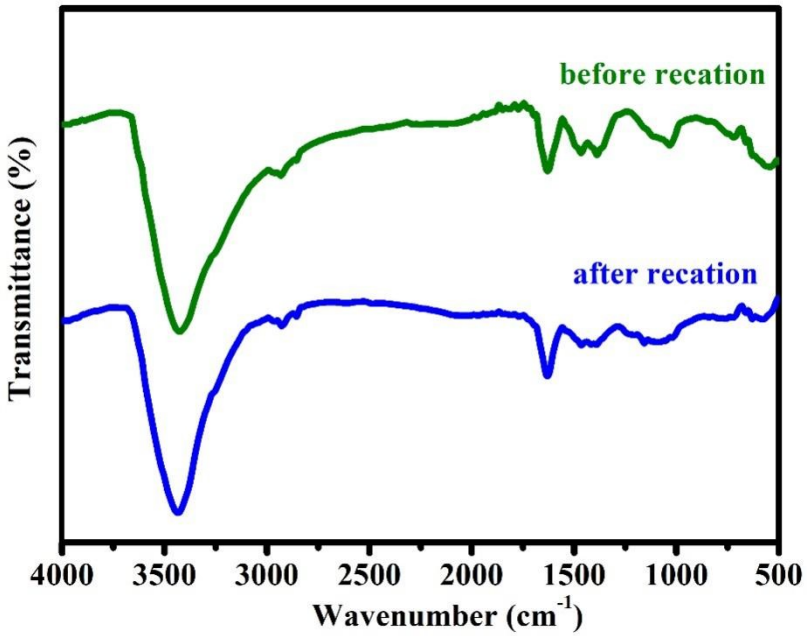

Fig. S8. FTIR spectra of ZnCdS(EDA)/Ni@NiO-3 before and after the reaction.

Fig. S9. SEM spectra of ZnCdS(EDA)/Ni@NiO-3

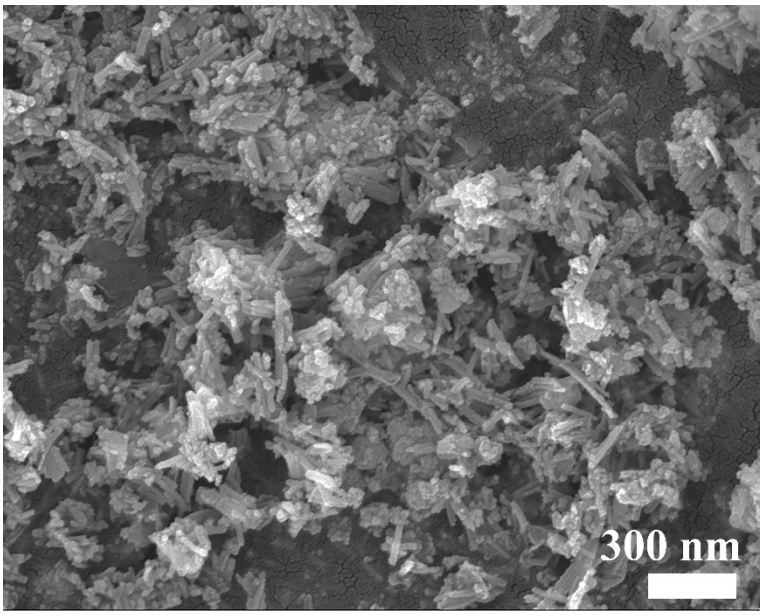

Fig. S9. SEM spectra of ZnCdS(EDA)/Ni@NiO-3 before and after the reaction.

Fig. S10. XPS spectrum of ZnCdS(EDA)/Ni@NiO-3

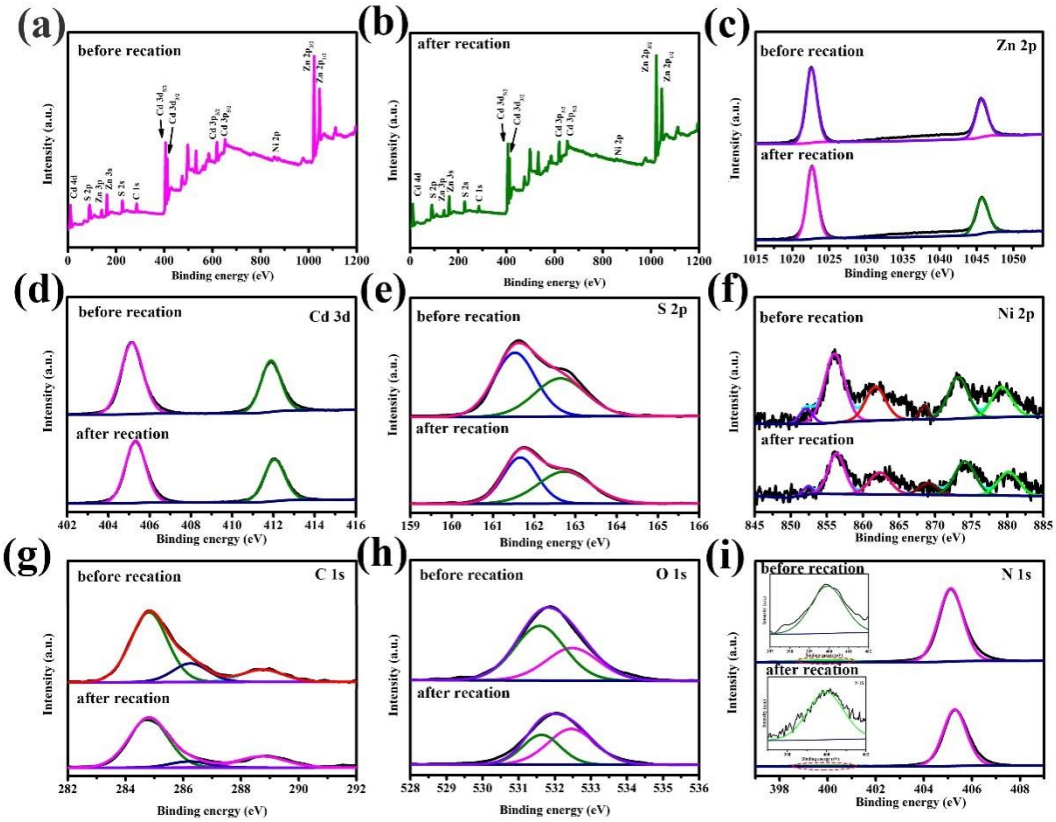

Fig. S10. XPS spectrum of ZnCdS(EDA)/Ni@NiO-3 before and after reaction: (a) XPS total spectrum of ZnCdS(EDA)/Ni@NiO-3 before reaction; (b) XPS total spectrum of ZnCdS(EDA)/Ni@NiO-3 after reaction; (c) XPS spectrum of Zn 2p; (d) XPS spectrum of Cd 3d; (e) XPS spectrum of S 2p; (f) XPS spectrum of Ni 2p; (g) XPS spectrum of C1s; (h) XPS spectrum of C1s; (i) XPS spectrum of N 1s.

Table S3. E_g, E_{VB} and E_{CB} results of different samples

Photocatalyst	E_g (eV)	E_{VB} (eV)	E_{CB} (eV)
ZnCdS(WAT)	2.24	-0.77	1.47
ZnCdS(EDA)	2.54	-0.79	1.75
NiO	3.5	-0.5	3.0

References

[1] H.F. Ye, R. Shi, X. Yang, W.F. Fu, Y. Chen, P-doped $Zn_xCd_{1-x}S$ solid solutions as photocatalysts for hydrogen evolution from water splitting coupled with photocatalytic oxidation of 5-hydroxymethylfurfural, Appl. Catal. B 233 (2018) 70-79.

[2] X.F. Ning, J. Li, B.J. Yang, W.L. Zhen, Z. Li, B. Tian, G.X. Lu, Inhibition of photocorrosion of CdS via assembling with thin film TiO_2 and removing formed oxygen by artificial gill for visible light overall water splitting, Appl. Catal. B 212 (2017) 129-139.

[3] C. Zhu, C.G. Liu, Y.J. Zhou, Y.J. Fu, S.J. Guo, H. Li, S.Q. Zhao, H. Huang, Y. Liu, Z.H. Kang, Carbon dots enhance the stability of CdS for visible-light-driven overall water splitting, Appl. Catal. B 216 (2017) 114-121.

[4] H. He, J. Cao, M.N. Guo, H.L. Lin, J.F. Zhang, Y. Chen, S.F. Chen, Distinctive ternary CdS/Ni_2P/g-C_3N_4 composite for overall water splitting: Ni_2P accelerating separation of photocarriers, Appl. Catal. B 249 (2019) 246-256.

[5] X.F. Ning, W.L. Zhen, Y.Q. Wu, G.X. Lu, Inhibition of CdS photocorrosion by Al_2O_3 shell for highly stable photocatalytic overall water splitting under visible light irradiation, Appl. Catal. B 226 (2018) 373-383.

[6] Y.Y. Zhong, Y.Z. Wu, B. Chang, Z.Z. Ai, K. Zhang, Y.L. Shao, L. Zhang, X.P. Hao, CoP/CdS/WS_2 p-n-n tandem heterostructure: a novel photocatalyst for hydrogen evolution without using sacrificial agents, J. Mater. Chem. A 7 (2019) 14638-14645.

[7] Y.J. Yuan, D.Q. Chen, S.H. Yang, L.X. Yang, J.J. Wang, D.P. Cao, W.G. Tu, Z.T. Yu, Z.G. Zou, Constructing noble-metal-free Z-scheme photocatalytic overall water splitting systems using MoS_2 nanosheets modified CdS as a H_2 evolution photocatalyst, J. Mater. Chem. A 5 (2017) 21205-21213.

[8] W. Li, X.S. Chu, F. Wang, Y.Y. Dang, X.Y. Liu, T.h. Ma, J.Y. Li, C.Y. Wang, Pd single-atom decorated CdS nanocatalyst for highly efficient overall water splitting under simulated solar light, Appl. Catal. B 304 (2022) 121000.

[9] J. Zhang, S. Z. Qiao, L.F. Qi, J.G. Yu, Fabrication of NiS modified CdS nanorod p–n junction photocatalysts with enhanced visible-light photocatalytic H-production activit, Phys. Chem. Chem. Phys. 15 (2013) 12088-12094.

[10] T.M. Di, Q.R. Deng, G.M. Wang, S.G. Wang, L.X. Wang, Y.H. Ma, Photodeposition of CoO_x and MoS_2 on CdS as dual cocatalysts for photocatalytic H2 production, J. Mater. Sci. Technol. 2022.

[11] Y.L. Jia, Z.Z. Wang, X.Q. Qiao, L. Huang, S.L. Gan, D.F. Hou, J. Zhao, C.H. Sun, D.S. Li, A synergistic effect between S-scheme heterojunction and Noble-metal free cocatalyst to promote the hydrogen evolution of ZnO/CdS/MoS2 photocatalyst, Chem. Eng. J. 424 (2021) 130368.

[12] Y.T. Ren, T.N. Dong, S.P. Ding, X.F. Liu, H.Z. Zheng, L.L. Gao, J.C.Hu, AgBr Nanoparticles Anchored on CdS Nanorods as Photocatalysts for H_2 Evolution, ACS Appl. Nano Mater. 4 (2021) 9274-9282.

[13] C.H. Li, H.G. Wang, S.B. Naghadeh, J.Z. Zhang, P.F. Fang, Visible light driven hydrogen evolution by photocatalytic reforming of lignin and lactic acid using one-dimensional NiS/CdS nanostructures, Appl. Catal. B 227 (2018)229-239.

[14] Y. Liu, H.T. Niu, W. Gu, X.Y. Cai, B.D. Mao, D. Li, W.D. Shi, In-situ construction of hierarchical CdS/MoS_2 microboxes for enhanced visible-light photocatalytic H_2 production, Chem. Eng. J. 339 (2018) 117-124.

[15] S. Wang, B.C. Zhu, M.J. Liu, L.Y. Zhang, J.G. Yu, M.H. Zhou, Direct Z-scheme ZnO/CdS hierarchical photocatalyst for enhanced photocatalytic H_2-production activity, Appl. Catal. B 243 (2019) 19-26.